DOI: 10.1007/s11099-015-0167-5 PHOTOSYNTHETICA 54 (1): 110-119, 2016

Effect of copper oxide nanoparticles on growth, morphology, photosynthesis, and antioxidant response in *Oryza sativa*

M.V.J. DA COSTA and P.K. SHARMA+

Department of Botany, Goa University, Goa, India 403 206

Abstract

The physiological and biochemical behaviour of rice (*Oryza sativa*, var. Jyoti) treated with copper (II) oxide nanoparticles (CuO NPs) was studied. Germination rate, root and shoot length, and biomass decreased, while uptake of Cu in the roots and shoots increased at high concentrations of CuO NPs. The accumulation of CuO NPs was observed in the cells, especially, in the chloroplasts, and was accompanied by a lower number of thylakoids per granum. Photosynthetic rate, transpiration rate, stomatal conductance, maximal quantum yield of PSII photochemistry, and photosynthetic pigment contents declined, with a complete loss of PSII photochemical quenching at 1,000 mg(CuO NP) L^{-1}. Oxidative and osmotic stress was evidenced by increased malondialdehyde and proline contents. Elevated expression of ascorbate peroxidase and superoxide dismutase were also observed. Our work clearly demonstrated the toxic effect of Cu accumulation in roots and shoots that resulted in loss of photosynthesis.

Additional key words: ascorbate; nanoparticle; proline; superoxide dismutase; thylakoid.

Introduction

Development of new nanomaterials and their application in various industrial uses results in greater pollution of the environment by nanoparticles (NPs) (Corredor *et al*. 2009). In recent years, NPs with sizes typically below 100 nm have been applied in an increasing number of commercial applications (Corredor *et al*. 2009), such as electronics, optics, textiles, medicine, catalysts, water treatment, and environmental remediation (Zhang and Elliot 2006). In 2005, the total global investment in nanotechnology was $10 billion and is set to reach $1 trillion by 2015 (Harrison 2007), leading to further increase of engineered NPs released into our environment. Manufactured NPs enter the environment unintentionally through atmospheric emissions, domestic waste water, agriculture, and accidental release during manufacture and transport (Klaine *et al*. 2008). This ultimately leads to NPs entry into soil and water bodies thereby affecting plants and animals. Due to their physical and chemical properties, NPs also interact with living systems. Studies on the interaction of NPs with the environment are being carried out in order to shed light on questions regarding size, structure, and reactivity in aquatic and sedimentary systems, their association with other colloids and behaviour in comparison to bulk counterparts (Klaine *et al*. 2008). However, the toxic potential of NPs to plants and their bioavailability are yet to be investigated (Klaine *et al*. 2008).

Metallo–NPs differ from bulk counterparts in surface characteristics, such as copious reactive sites and mobility regulated by deposition or aggregation (Maynard *et al*. 2006) which is in turn dependent on pH, temperature, particle size, ionic strength, and concentration (Wiesner

Received 8 February 2015, *accepted* 29 June 2015, *published as online-first* 10 August 2015.
+Corresponding author; phone: 0832 6519346, fax: 0832 2451184, e-mail: prabhat_k_sharma@rediffmail.com
Abbreviations: AAS – atomic absorption spectrophotometer; APX – ascorbate peroxidase; DM – dry mass; *E* – transpiration rate; FM – fresh mass; F_m – maximum fluorescence; F_o – initial fluorescence; F_s – steady-state fluorescence; F_v/F_m – maximal quantum yield of PSII photochemistry; GR – glutathione reductase; g_s – stomatal conductance; IRGA – infra red gas analyser; MDA – malondialdehyde; NP(s) – nanoparticle(s); P_N – photosynthetic rate; q_P – photochemical quenching; ROS – reactive oxygen species; SEM – scanning electron microscope; SOD – superoxide dismutase; TBA – thiobarbituric acid; TEM – transmission electron microscope; XRD – X-ray diffraction.
Acknowledgements: We thank the Department of Science & Technology (DST), New Delhi (SR/SO/PS–63/2009) and UGC– SAP (F. 3–50/2009 (SAP–II) for funding this work. We would like to thank All India Institute of Medical Sciences, New Delhi for TEM imaging; NIO, Goa for SEM imaging and atomic absorption spectrophotometry; Physics Department, Goa University for NP size determination using X-ray diffractometer. We are grateful to Andrew Willis, Centre for Agroecology, Water and Resilience (CAWR), Coventry University, Coventry, United Kingdom for correcting the English of the manuscript.
Both authors made equal contribution to the work presented in this paper.

et al. 2006). These characteristics lead to electrostatic, hydrogen bonding, and hydrophobic interactions with structural and catalytic proteins in the cell (Ojamäe *et al*. 2006). Literature states that NPs exist as colloids at low concentrations and may form small stable aggregates at moderate concentrations (Klaine *et al*. 2008), while a small amount of metallo–NPs may also dissociate into ions (Navarro *et al*. 2008). The mechanism of NP uptake by plant roots is not clearly understood. Studies have shown that, depending on the size, NPs may enter the plant cell through carrier proteins, aquaporins, ion channels, *via* fluid phase endocytosis, plasmodesmata transport, or entry may be facilitated through natural organic matter or root exudates and formation of new pores (Rico *et al*. 2011).

Copper is an essential micronutrient required for the normal growth of plants. It is involved in many physiological processes as it exists in multiple oxidative states (Cu^{2+}, Cu^{+}) *in vivo* (Yruela 2005). It acts as a structural component in regulatory proteins and in those involved in photosynthetic electron transport, mitochondrial respiration, oxidative stress responses, cell wall metabolism, and hormone signalling (Marschner 1995, Raven *et al*. 1999, Solymosi and Bertrand 2012). At the cellular level, Cu plays an important role in signalling of transcription, protein trafficking machinery, oxidative phosphorylation, and iron mobilization as well. The redox property of Cu can also contribute to its toxicity, as free ions catalyse the production of damaging radicals (Manceau *et al*. 2008). No published data are available on the concentration of metallo–NPs including CuO NPs in soil, however, heavy metal Cu is estimated to be in the range of 2–100 mg kg^{-1}(DM) in typical uncontaminated soils (Nagajyoti *et al*. 2010).

In recent years, significant research has been focused on studying CuO NPs effects in plants. The limit of metal NP accumulation, across a range of metals, is proposed to be controlled by the total reducing capacity of the plant (Haverkamp and Marshall 2009). It is reported that the exposure to Cu NP (50 nm) at concentration of 1,000 mg L^{-1} in *Cucurbita pepo* (zucchini) resulted in 90% biomass reduction (Stampoulis *et al*. 2009). Cu NPs were toxic to the growth of *Phaseolus radiatus* (mung bean) and *Triticum aestivum* (wheat) at concentrations up to 1,000 mg L^{-1} (Lee *et al*. 2008). Similarly, reduction in the growth and transpiration of *C. pepo* by 60–70% relative to untreated control was reported by Musante and White (2012) after treatment with CuO NPs. Available published data and the lack of knowledge on the metallo–NPs influence in plants is a major limitation which warrants extensive research on this topic.

Further studies, other than germination, root and shoot length, and biomass need to be carried out with regard to CuO NPs in order to understand better uptake, accumulation, and effects on photosynthesis, and other physiological and biochemical processes in plants. Therefore, this study was conducted to examine the effect of CuO NPs on *Oryza sativa* plants grown hydroponically at concentrations ranging from 0–1,000 mg L^{-1} (w/v) on the growth, accumulation of Cu in leaves and roots, external and internal morphology, photosynthesis, oxidative and osmotic stress, and expression level of antioxidant genes, such as ascorbate peroxidase (APX) and superoxide dismutase (SOD).

Materials and methods

Plant material and treatments: *Oryza sativa* (var. Jyoti), a high yielding rice variety, was obtained from Indian Council of Agricultural Research, Goa and stored in dark at 20°C. CuO NPs (<50 nm size, *Sigma–Aldrich*) was prepared in Hoagland's solution with concentrations of 0 (control), 2.5, 10, 50, 100, and 1,000 mg L^{-1}(w/v) at pH 6.5. Seeds were surface sterilized using 4% sodium hypochlorite (*BDH*) solution, washed 5–6 times and soaked in tap water [Cu content < 0.06 mg L^{-1} (w/v)] for 3 d. Germination paper was placed in Petri dishes, rice seeds were sown, and a NP suspension of various concentrations was applied in respective Petri dishes. They were placed in a growth chamber under the temperature of 25 ± 2ºC with 16 h photoperiod and light intensity of 200 μmol(photon) m^{-2} s^{-1}. The 6-d-old seedlings were transferred carefully into the hydroponic system and grown for further 24 d. The hydroponic system ensured complete mixing of NPs by use of magnetic stirrers and proper aeration was achieved by air pumps. The solutions were changed with respective NP solutions every third day.

Nanoparticle size determination: Scanning electron microscope (SEM, *JSM 5800 LV, JEOL,* Japan) operating at a constant acceleration voltage of 10 kV was used to characterize CuO NPs. NPs were ultra-sonicated in 100% ethanol and a drop of this solution was placed onto the stub layered with carbon conductive, double sided adhesive tape (*SPI Supplies*®, USA). The sample was air-dried and sputter coated with gold for 15 s (*SPI-MODULE Gold Sputter Coater*) under high vacuum at the National Institute of Oceanography, Goa. Further confirmation of the particle size was done using X-ray diffractometer (*XRD ultraX 18HB–300, Rigaku,* Japan) with a scintillation counter probe *SC-30*. CuO NP powder was directly mounted on sample holders and the X-ray diffraction XRD pattern was recorded at room temperature in the range of 2 θ = 20°–80° with a step of 0.02° and 2° min^{-1} speed using Cu kα radiation (λ = 0.15406 nm). The data analysis was performed using *Traces* software (*GBC Scientific Instruments*, USA) and the particle size was determined using Scherrer's formula considering the first three peaks of the pattern obtained.

Growth, morphology and biomass studies: Percentage of germination, shoot and root length were measured after 6 d. The biomass was measured in 10 randomly selected plants grown in CuO NPs after 30 d. The external leaf and root morphology was studied by visualizing lyophilized segments using SEM (*JSM 5800 LV, JEOL*, Japan). The internal leaf and root morphology was studied using transmission electron microscopy (TEM) at All India Institute of Medical Sciences (AIIMS), New Delhi. The leaf and root tissue was cut into 2 × 2 mm pieces and fixed in a mixture of 2% paraformaldehyde and 2.5% glutaraldehyde in 0.1 M phosphate buffer for 10:00 h at 4°C. The tissue samples were washed in 0.1 M phosphate buffer at 4°C. Samples were then postfixed at room temperature for 1 h in 1% OsO_4 in 0.1 M phosphate buffer (pH 7.2). Samples were dehydrated in acetone, infiltrated, and embedded in *Araldite CY 212*. Thin, serial sections were cut (70–80 nm thick) using ultramicrotome (*Leica UC6, Leica Microsystems*, Germany), collected on copper grids, stained with uranyl acetate and lead citrate, and examined under a TEM (*Morgagni 268D, Fei Company*, The Netherlands).

Nanoparticle uptake: Uptake of NPs was determined using atomic absorption spectrophotometer (*Flame Furnace system–AAnalyst 200*, AAS*, Perkin Elmer,* USA). The ash was dissolved in 1% HNO_3 (*Merck*) solution and filtered through 0.45 µm Whatman filter paper and then used. The filtered sample was used for AAS analysis in whole root and leaf tissues, as well as in different sections of the leaf (apical, middle, and basal region) at different concentrations of CuO NPs.

Carbon dioxide fixation: Studies were carried out using a portable infrared gas analyser (*ADC Bioscientific, LCi–SD, Hansatech*, UK) using inbuilt software as described by Sharma and Hall (1996). The photosynthetic rate (P_N), transpiration rate (E), and stomatal conductance (g_s) were measured at ambient temperature, CO_2 concentration, and light intensity of 1,200 µmol(photon) m^{-2} s^{-1} using a detachable light source provided by a dichroic lamp (*Hansatech*, UK).

Chlorophyll (Chl) fluorescence measurements were carried out according to Sharma *et al*. (1997) using a fluorescence monitoring system (*FMS–1, Hansatech*, UK). The leaf samples were dark adapted for 10 min to inhibit all light-dependent reactions by completely oxidizing PSII electron acceptor molecules. A weak modulating beam of intensity 3–4 µmol(photon) m^{-2} s^{-1} was focused on the sample to measure initial fluorescence (F_o), followed by exposure to a saturating pulse [approximately 4,000 µmol(photon) m^{-2} s^{-1} for 0.06 s] to measure the maximum fluorescence (F_m). Variable fluorescence (F_v) was determined by substracting F_o from F_m as ($F_v = F_m - F_o$) and the maximum quantum yield (F_v/F_m) ratio was calculated. Actinic light was provided at an intensity of 1,200 µmol(photon) m^{-2} s^{-1} and allowed to reach a steady-state fluorescence yield (F_s) after which far red pulse was given for 5 s. It was then used to calculate the relative contributions for photochemical and nonphotochemical energy dissipation measured as the photochemical quenching (q_P) and nonphotochemical quenching (q_N) using *Modfluor32* software.

Extraction and analysis of photosynthetic pigments: Leaf tissue (0.1 g) was ground in 100% acetone (*Merck*, HPLC grade) making a final volume of 1.5 ml and incubated overnight at 4ºC. The homogenate was centrifuged (*Z32HK, HERMLE Labortechnik GmbH,* Germany) at 4ºC for 10 min at 4,000 × *g*. One ml of supernatant was collected and filtered through 0.2 µm *Ultipor®N66®Nylon* membrane filter (*PALL Life Sciences,* USA) and 10 µl of sample was analysed in an HPLC system (*Waters,* USA), using two–solvent gradient as a mobile phase (using *Merck* HPLC grade chemicals) composed of solution A (ethyl acetate) and solution B (acetonitrile:water, 9:1). The mobile flow rate was 1.2 ml min^{-1} for a run time of 30 min. The pigments were separated using a C18 column (*Waters Spherisorb* ODS2 – 250 mm × 4.6 mm × 5 µm). The pigment peaks were determined at 445 nm with a *Waters 2996* photodiode array detector based on RT and spectral characteristics. β–carotene was used as an external standard for quantification of pigments (Sharma and Hall 1996).

Lipid peroxidation was determined by estimation of the malondialdehyde (MDA) content in leaves following Sankhalkar and Sharma (2002). The amount of MDA (extinction coefficient of 155 mM^{-1} cm^{-1}) was calculated by subtracting nonspecific absorbance at 600 nm from absorbance at 532 nm using UV-Visible spectrophotometer (*UV–2450, Shimadzu*, Singapore).

Proline determination: Proline accumulation in fresh leaves was determined according to the method of Bates *et al*. (1973); the absorbance at 520 nm was measured using UV-Visible spectrophotometer (*UV–2450*, *Shimadzu*, Singapore). L-proline (*Sigma*) was used as standard.

Ascorbate assay: Estimation of ascorbate (ASA) in fresh leaves was carried out according to the method of Kampfenkel *et al*. (1995); the absorbance at 520 nm was measured using UV-Visible spectrophotometer (*UV-2450, Shimadzu*, Singapore). Ascorbic acid (*Himedia*) was used as standard.

RNA extraction and quantification and gene expression studies: Leaf tissue (0.1 g) was ground using liquid nitrogen and extracted using the protocol mentioned in the RNA extraction kit (*Invitrogen*). The RNA extracted was quantified using a spectrophotometer at 260 and 280 nm (*UV–2450, Shimadzu*, Singapore).

cDNA preparation using RT PCR: cDNA synthesis was done using PCR kit (*Invitrogen* Superscript III Reverse Transcriptase, Cat no: 18080/093/044/085) following the given protocol.

Real time analysis using Real time PCR: Expression of genes for antioxidant enzymes ascorbate peroxidase (APX) and superoxide dismutase (SOD) was studied using *MJ Miniopticon* real time PCR system, *Bio-Rad,* USA. *APX* primers (Oligo number: 91211B3–1255C12 17/44) APX–Thy–L 5'– GCT AAA CTG AGC GAC CTT GG –3', (Oligo number: 91211B3–1255D12 18/44) APX–Thy–R 5'– GCT GCT CCT ACC GTT ACT GG –3' and *SOD* primers (Oligo number: 30121B3–9644D10 5/32) SOD–F 5'–CGT CGA TCT CCC ATC ATT TT–3', (Oligo number: 30121B3–9644E10 6/32) SOD–R 5'–CTT GTT CCG TTT TGT GTG GA–3' were procured from *Pharmaids and Equipments Pvt. Ltd*., India. Reaction was followed in 50 µl of total volume using the *Bio-Rad* kit protocol (*SsoAdvanced SYBR Green Supermix*, cat no.: 172–5260). Amplification was carried out for 40 cycles. Data were analysed using *Bio-Rad CFX manager* software.

Statistical analysis: The data shown corresponded to the mean values ± standard deviation (SD). One-way analysis of variance (*ANOVA*) and *Duncan*'s multiple range test by using *Microsoft Excel XLSTAT* (*version 2015.2.01.17315*) were performed to confirm the variability of the results and the determination of significant ($P \leq 0.05$) difference between treatment groups, respectively.

Results

The NP characterization studies revealed that the shape of CuO NPs was spherical and the size was estimated as < 50 nm using SEM (Fig. 1*A*) and applying Scherer's formula to the X-ray diffraction (XRD) data (Fig. 1*B*).

The germination rate of rice plants was slightly affected (7%) at 1,000 mg L^{-1} CuO NPs compared with control (Table 1). During the early stage of growth (6 d old), the plantlets showed a decrease in root (23%) and shoot (31%) length compared with the control at higher concentrations (Table 1). The decrease in root and shoot growth was found when the plants were treated with 100 mg L^{-1} CuO NPs and higher concentrations (Table 1). Biomass of rice shoots grown at 1,000 mg L^{-1} CuO NP decreased by 31% on fresh mass (FM) basis and 14% on a dry mass (DM) basis. Root biomass increased by 9% at 1,000 mg L^{-1} CuO NP when calculated on FM basis but decreased by 16% on DM basis (Table 1) compared with the control.

The effect of CuO NPs on leaf and root surface studied using SEM showed an increase in the number of trichomes (Fig. 2*A,B,C*) and a decrease in the number (Fig. 2*A,B,C*) and size of stomata (Fig. 2*D,E,F*). External damage to the root surface was also observed at 1,000 mg L^{-1} CuO NPs (Fig. 2*G,H,I*).

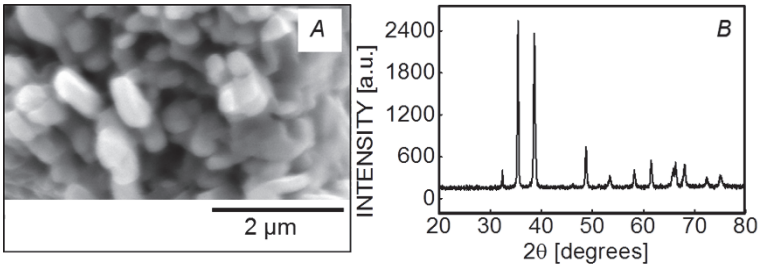

Fig. 1. SEM image of CuO NPs at a magnification of 30,000 × (*A*) and X-ray diffraction pattern (*B*) of CuO NPs recorded at room temperature in the range 2θ = 20°–80° with a step of 0.02°, speed = 2°min^{-1} using Cu kα radiation (ʎ = 0.15406 nm).

Table 1. Percentage of germination, shoot, root length, and biomass (fresh mass – FM, and dry mass – DM) of *Oryza sativa* treated with CuO nanoparticles (NPs) at different concentrations. Mean values ± SD ($n = 5$). Means in the column followed by the *same letter* do not differ significantly at $p \leq 0.05$.

NPs [mg L^{-1}]	Germination [%]	Shoot length [mm]	Root length [mm]	Shoot biomass [g]		Root biomass [g]	
				FM	DM	FM	DM
0	96.0 ± 3.97^{a}	35.2 ± 6.36^{ab}	48.4 ± 6.33^{a}	0.64 ± 0.01^{a}	0.087 ± 0.05^{c}	0.192 ± 0.02^{c}	0.025 ± 0.01^{a}
2.5	94.7 ± 3.10^{ab}	31.0 ± 1.22^{bc}	45.8 ± 5.96^{a}	0.64 ± 0.02^{a}	0.092 ± 0.03^{a}	0.193 ± 0.03^{c}	0.021 ± 0.02^{e}
10	90.1 ± 1.86^{bc}	27.8 ± 1.64^{cd}	43.8 ± 6.89^{ab}	0.63 ± 0.02^{a}	0.087 ± 0.02^{b}	0.205 ± 0.02^{b}	0.021 ± 0.01^{e}
50	89.7 ± 6.61^{c}	39.0 ± 3.36^{a}	48.5 ± 2.88^{a}	0.61 ± 0.02^{a}	0.078 ± 0.01^{d}	0.188 ± 0.02^{d}	0.023 ± 0.01^{c}
100	89.2 ± 4.53^{c}	25.7 ± 3.36^{d}	42.2 ± 3.53^{ab}	0.43 ± 0.01^{b}	0.071 ± 0.03^{f}	0.180 ± 0.02^{e}	0.024 ± 0.01^{b}
1000	88.7 ± 4.82^{c}	24.3 ± 3.12^{d}	37.2 ± 4.35^{b}	0.44 ± 0.05^{b}	0.075 ± 0.02^{e}	0.209 ± 0.01^{a}	0.021 ± 0.01^{d}

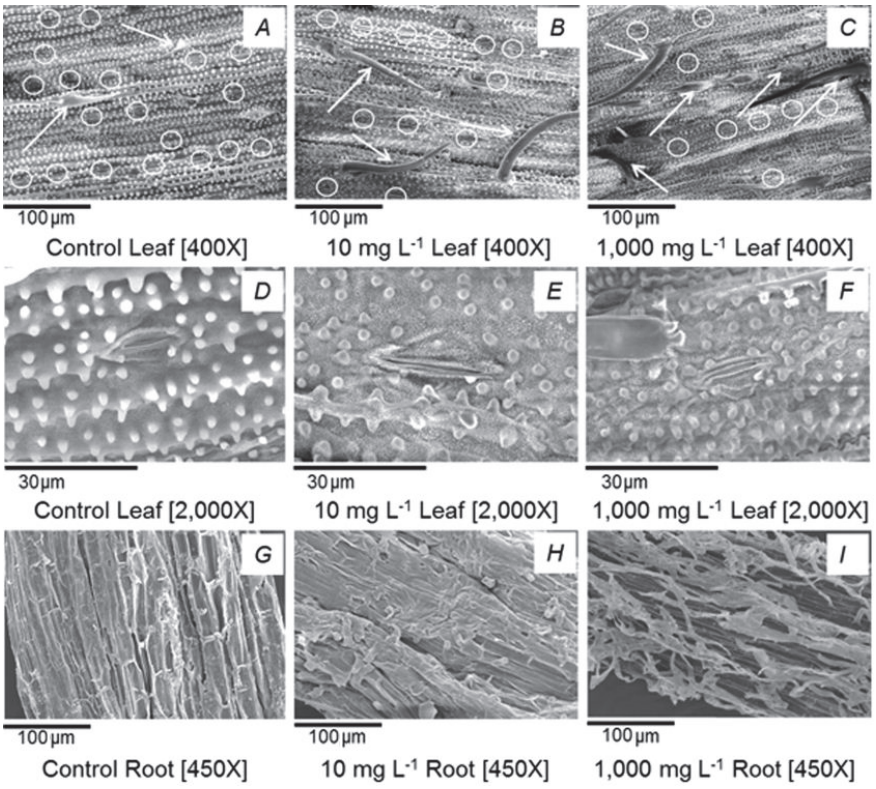

Fig. 2. SEM images of leaf (adaxial) surface showing trichomes (*A–C*), stomata (*D–F*), and roots (*G–I*) of plants treated with CuO nanoparticless for 30 d. *The arrows* indicate trichomes and *the circles* represent stomata.

TEM micrographs showed accumulation of CuO NPs inside the leaf and root cells (Fig. 3*A–C*). Accumulation of NP in the leaf was especially observed in the chloroplasts. The treatments resulted in the reduced number of thylakoids per granum at the concentration higher than 50 mg L^{-1}; a distortion (wavy arrangement) of the thylakoid membranes and swelling of the intra-thylakoidal space was observed at 1,000 mg L^{-1} CuO NPs (Fig. 3*D–F*).

Cu accumulation in the whole leaf and all leaf segments increased at the high concentration of CuO NPs (Table 2). The increase of 5.5–fold in the Cu content was observed in the whole leaves treated with 1,000 mg L^{-1} CuO NP as compared with the control plants. The increase of 76-fold in the Cu content was observed in the whole roots treated with 100 mg L^{-1}. At the highest concentration, however, Cu accumulation in the whole root tissue was only 9.4-fold as compared with the control (Table 2). Leaf segments (apical, middle, and basal region) analysed for the Cu content showed the

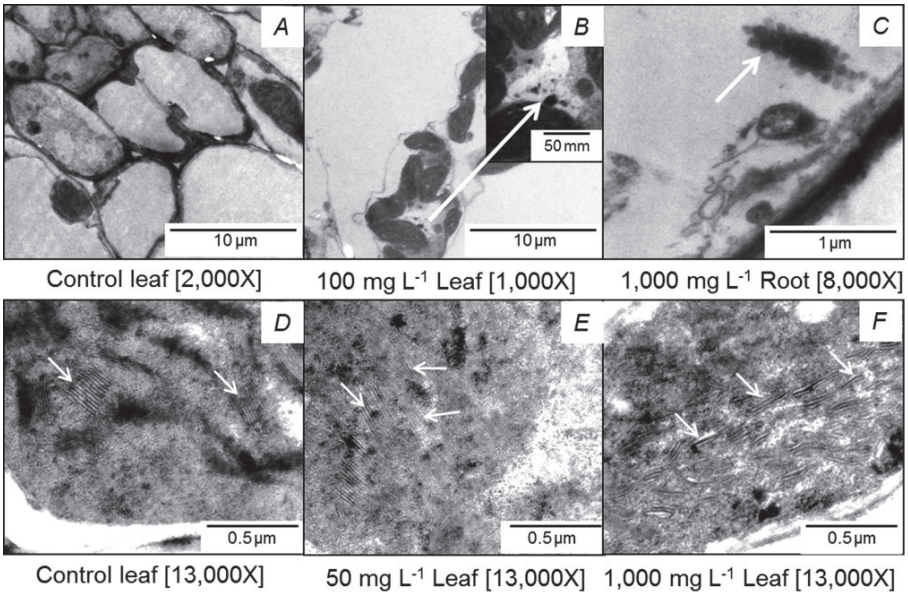

Fig. 3. TEM images of leaf showing the accumulation of CuO nanoparticles in chloroplast (*A,B*), in root (*C*), and reduction in chloroplast thylakoid stacking and appearance of the particles in chloroplast (*D–F*). *The arrows* indicate CuO nanoparticles (*B–C*) and changes in thylakoid stacking (*D–F*).

Table 2. Cu content in leaves and roots of *Oryza sativa* plants treated with CuO nanoparticles (NPs) at concentrations of 0–1,000 mg L^{-1} for 30 d. Mean values ± SD (n = 3). Means in the column followed by *the same letter* do not differ significantly at $p \leq 0.05$.

CuO NPs [mg L^{-1}]	Cu in leaf [mg kg^{-1}(DM)]				Cu in root [mg kg^{-1}(DM)]
	Whole leaf tissue	Apical region	Middle region	Basal region	Whole root tissue
0	3.12 ± 0.14^{d}	3.44 ± 0.3^{d}	5.15 ± 0.15^{c}	4.50 ± 0.4b^{c}	20.21 ± 2.0^{e}
2.5	5.0 ± 0.21^{c}	3.64 ± 0.1^{d}	3.42 ± 0.3^{c}	3.21 ± 1.4^{c}	289.0 ± 10.2^{d}
10	5.36 ± 0.32^{c}	3.57 ± 0.26^{d}	3.70 ± 0.3^{c}	3.49 ± 0.9^{c}	559.9 ±14.9^{c}
50	5.9 ± 0.36^{bc}	6.20 ± 0.6^{c}	5.45 ± 0.26^{c}	6.43 ± 0.1^{b}	753.2 ±11.7^{b}
100	6.65 ± 0.50^{b}	8.50 ± 0.45^{b}	8.27 ± 1.22^{b}	6.97 ± 0.1^{b}	1,544.1 ± 18.9^{a}
1,000	17.27 ± 1.45^{a}	14.11± 0.9^{a}	14.36 ± 3.3^{a}	21.30 ± 3.3^{a}	190.14 ± 10.95^{f}

highest accumulation at 1,000 mg L^{-1}. No specific pattern of accumulation was found in apex, middle, and basal segments of leaves (Table 2).

A significant decrease was observed in P_N, E, and g_s at high concentrations of CuO NPs (Fig. 4*A*). The decrease of 86% in P_N was observed in the plants treated with 1,000 mg L^{-1} CuO NPs. The similar decrease was also observed in E and g_s (Fig. 4*A*). The maximum quantum efficiency of PSII measured as F_v/F_m ratio did not significantly differ from control up to 10 mg L^{-1} of CuO NPs. At 1,000 mg L^{-1}, a decrease of 46% was observed compared with the control (Fig. 4*B*). The photochemical quenching (q_P) showed no change up to the 100 mg L^{-1} CuO NPs, but it significantly diminished at 1,000 mg L^{-1} (Fig. 4*B*). Nonphotochemical quenching (q_N) showed a slight increase (10%) at 1,000 mg L^{-1} compared with the control (Fig. 4*B*).

The Car (violaxanthin, lutein, and *β*–carotene) content increased by more than 50% at 2.5 mg L^{-1} CuO NPs, but higher concentrations of the NPs resulted in a significant decrease in the pigment content (Table 3). Violaxanthin increased by 95% at 2.5 mg L^{-1} and decreased by more than 58% at concentrations of 100 mg L^{-1} and above. The lutein content increased by 67% at 2.5 mg L^{-1}, but decreased linearly to 70% at 1,000 mg L^{-1} compared with the control. The *β*–carotene content showed no change up to 10 mg L^{-1}, decreasing by 90% at high concentrations (1,000 mg L^{-1} CuO NPs). Similarly, the Chl *a*/*b* ratio showed no change up to 10 mg L^{-1}, but it increased by 41% at 1,000 mg L^{-1}.

We observed a negligible difference in lipid peroxidation, measured as MDA–TBA adducts, up to 1,000 mg L^{-1} CuO NPs (Fig. 5*A*). Proline increased up to 2.2 times of the control with 1,000 mg L^{-1} CuO NPs (Fig. 5*B*). Similarly, ascorbate, which acts as a nonenzymatic antioxidant, increased by 30% compared with the control in leaves of plants treated with CuO NP at the high concentration (Fig. 5*C*).

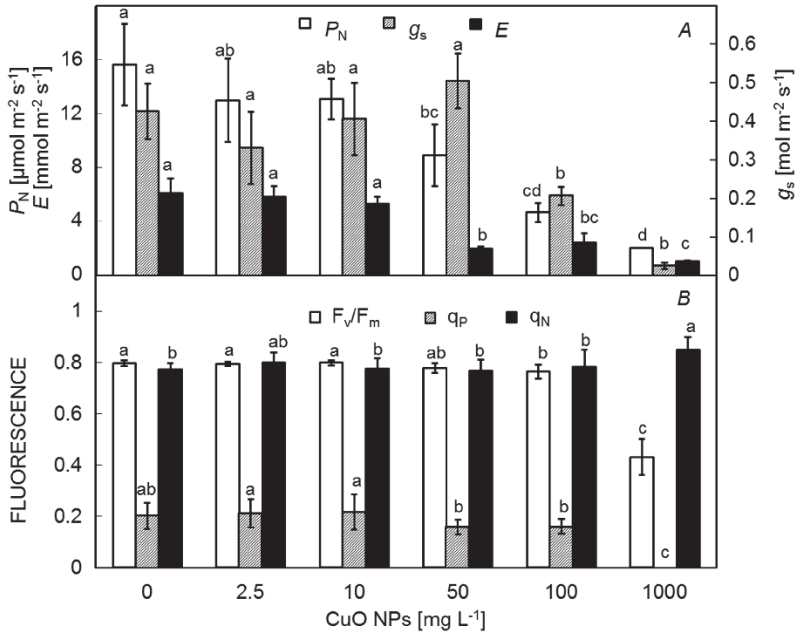

Fig. 4. Photosynthetic rate (P_N), stomatal conductance (g_s), and transpiration rate (E) (*A*) and photosynthetic efficiency of PSII (F_v/F_m), photochemical quenching (q_P), and nonphotochemical quenching (q_N) (*B*) of rice plants treated with CuO NPs for 30 d. Mean values ± SD (n = 5). Means in the column followed by *the same letter* do not differ significantly at $p \leq 0.05$.

Table 3. Carotenoid (Car) content and relative chlorophyll (Chl) content of *Oryza sativa* leaves treated with CuO nanoparticles (NPs) at concentrations of 0–1,000 mg L^{-1} for 30 d. Mean values ± SD (n = 3). Means in the row followed by *the same letter* do not differ significantly at $p \leq 0.05$. The ratio was calculated taking mean values of the respective pigments.

Pigment content [μg g^{-1}(FM)]	CuO NPs [mg L^{-1}]				
	0	2.5	10	100	1,000
Violaxanthin	1.3 ± 0.001^b	2.4 ± 0.06^a	1.0 ± 0.009^b	0.3 ± 0.001^c	0.5 ± 0.009^d
Lutein	2.3 ± 0.003^b	3.9 ± 0.07^a	2.1 ± 0.009^b	1.1 ± 0.007^c	0.7 ± 0.07^d
β–carotene	4.9 ± 0.30^a	5.3 ± 0.05^a	5.2 ± 0.09^a	1.5 ± 0.07^b	0.5 ± 0.02^c
Chl *a*/*b* ratio	1.46	1.51	1.50	1.7	2.06

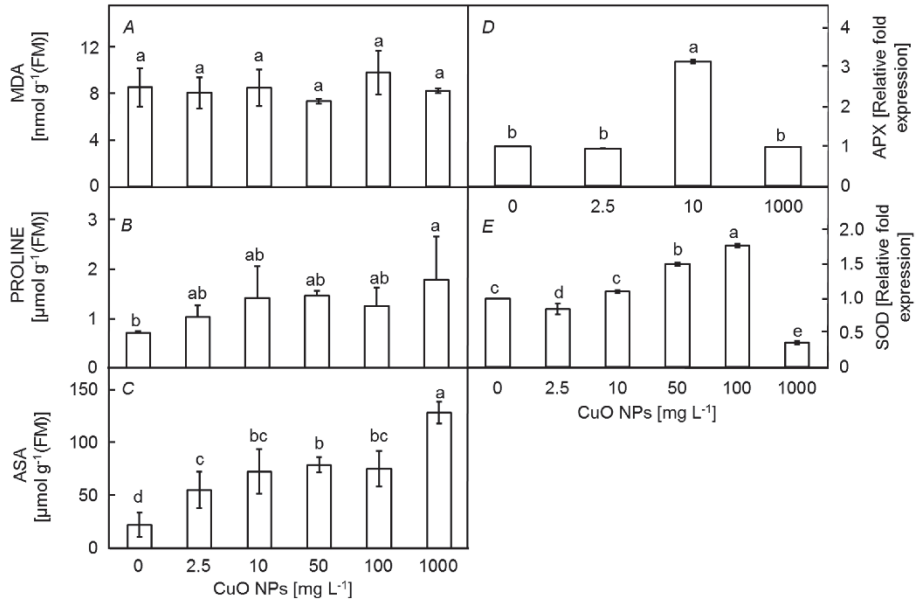

Fig. 5. Malondialdehyde (MDA) (*A*), proline (*B*), and ascorbate (ASA) contents (*C*) and the relative expression of ascorbate peroxidase (APX) (*D*) and superoxide dismutase (SOD) (*E*) in rice plants treated with CuO nanoparticles for 30 d. Mean values ± SD (n = 5). Means in the column followed by *the same letter* do not differ significantly at $p \leq 0.05$.

Gene expression of enzymatic antioxidants, such as ascorbate peroxidase (APX) and superoxide dismutase (SOD), increased with the increasing CuO NP concentration. APX showed a 3-fold increase in its gene expression at 10 mg L^{-1}. At 1,000 mg L^{-1} of CuO NP, gene expression level of APX was similar to that of control (Fig. 5*D*). SOD expression level increased to 1.5–fold at 50 mg L^{-1} CuO NP and doubled at 100 mg L^{-1} compared with the control. CuO NP at 1,000 mg L^{-1} showed a significantly decreased level of SOD expression to that observed in control (Fig. 5*E*).

Discussion

We observed negligible effect of CuO NPs on seed germination (Table 1); it might be due to a selective permeability that is exhibited by the seed coat. This protects the embryo from CuO NPs toxicity by restricting the entry of NPs until radicles emerge and come into a direct contact with the NPs in the growth medium. Wierzbicka and Obidzińska (1998) reported selective permeability of metallo–NPs. Our results are similar to those reported by Stampoulis *et al*. (2009) in *C. pepo* treated with 1,000 mg L^{-1} of Cu NPs of 50 nm size, and by Lee *et al*. (2010) with aluminium oxide (~150 nm size), silicon dioxide (42.8 nm size), and magnetite (< 50 nm size) NPs in *Arabidopsis thaliana*. Contrary to our results, CuO NPs are reported being toxic at concentrations as low as 1 mg L^{-1} in duckweeds (*Landoltia punctata*; Shi *et al*. 2011) and as high as 4,000 mg L^{-1} in buckwheat (*Fagopyrum esculentum*; Lee *et al*. 2013), indicating that the elemental composition, particle size, and concentration as well as plant species play an important role in NP toxicity on seed germination.

The reduced shoot and root length values observed in our study (Table 1) might result from accumulation of Cu in root and leaf tissues (Table 2). This was indicated by the massive increase of Cu in roots (76–fold) and leaves (5.5–fold) in comparison with the control (Table 2). Our results were in agreement with earlier work done by Lidon and Henriques (1998) on the effect of Cu on the shoot and root length. They reported that Cu at 0.25 and 1.25 mg L^{-1} caused a reduction in rice shoot length. Lee *et al*. (2008) showed that Cu NP caused a reduction in the

seedling length of *P. radiatus* and *T. aestivum* by 65% and 75%, respectively. Similarly, CuO NPs decreased root length in *C. pepo* at 1,000 mg L^{-1} concentration (Stampoulis *et al*. 2009).

Our results of SEM showed external morphological damage to the roots (Fig. 2*G–I*), reduced number (Fig. 2*A–C*) and size (Fig. 2*D–F*) of stomata, and increase of leaf trichomes (Fig. 2*A–C*). The damage to roots may have affected water uptake, leading to stomatal limitation and thereby limiting net photosynthesis (Fig. 4*A*). Kennedy and Gonsalves (1987) reported that Cu may adhere to the root surface leading to osmotic stress by decreasing the trans-root potential which is essential for water and ion uptake. Decline in root growth after a treatment with CuO NPs may also result in the reduction of surface area for water uptake, developing a negative water potential leading to osmotic stress (Alia and Pardha Saradhi 1991). The observed increase in the proline content (Fig. 5*B*), along with the decrease in the number and size of stomata and the increase in trichomes (Fig. 2), clearly indicated the development of osmotic stress due to the treatment. Similarly, the swelling of the intrathylakoidal space (Fig. 3*F*) is a phenomenon often associated with metal stress (Solymosi and Bertrand 2012) and has been also clearly associated with osmotic stress (Abdelkader *et al*. 2007, Ünnep *et al*. 2014).

Many feasible modes of NP uptake have been suggested but no experimental data are available on the actual mechanism. The AAS analyses revealed that accumulation of NPs in the roots greatly increased when compared to that of leaves (Table 2), indicating that only a small portion of NPs was transported from the roots to the shoots; thus, it led to major toxic effect in the roots. AAS analysis of Cu accumulation in the whole leaves as well as in apical, middle, and basal parts of leaves suggested nonspecific pattern of Cu accumulation. The greater metal content in roots than that in shoots indicates an exclusion mechanism to withstand toxicity; such plants accumulate metals in roots to prevent their transport to shoots (Wang *et al*. 2004). This accumulation may also occur due to large amount of mucilage secreted by the root tips and hairs contributing to the adsorption of NPs (Campbell *et al*. 1990, Zhang *et al*. 2011). Once adsorbed, NPs may not be available for transportation to shoots (Lin and Xing 2008). However, Lidon and Henriques (1998) observed that Cu accumulation in shoots of rice (*Oryza sativa* L. cv. Safari) increased with increasing Cu NP concentration, and accumulation was mainly found in shoot vacuoles. The decline in Cu accumulation in roots at 1,000 mg L^{-1} observed in this study might occur due to aggregation of CuO NPs at the root–medium interface (Song *et al*. 2015). Lee *et al*. (2008) also showed significant uptake of Cu NPs by *P. radiatus* and *T. aestivum* at 1,000 mg L^{-1}.

We observed the decline in P_N (Fig. 4*A*) that could result from various factors. The decrease in the number and size of stomata (Fig. 2*D–F*) as well as the decline in the photosynthetic pigments (Table 3) might result in the lower rate of photosynthesis (Fig. 4*A*). The decrease in g_s (Fig. 4*A*) might also result in the lowering of photosynthesis as well as *E* (Fig. 4*A*). The decrease in the thylakoid stacking (Fig. 3*E*) may also decrease the rate of photosynthesis and is often observed upon metal stress (Solymosi and Bertrand 2012). The decline in the number of thylakoids per grana is considered to be a result of reduced amount in PSII–LHCII complexes which play a crucial role in light-harvesting as well as ultrastructural organization of thylakoids; it may result in decreased Chl *a* fluorescence parameters (Kirchhoff *et al*. 2000). The increase in the Chl *a*/*b* ratio (Table 3) also indicated the reduced number of thylakoids per granum (A. Telfer, personal communication). The decrease in the number of thylakoids per granum may lower the quantum efficiency of photosynthesis (measured as F_v/F_m ratio) and q_P while increasing q_N (Fig. 4*B*). Photosynthesis has been reported to be supressed by CuO NPs in *Elodea densa* (Nekrasova *et al*. 2011) and duckweeds, *Landoltia punctata* (Shi *et al*. 2011). In another report, Saison *et al*. (2010) showed that core–shell CuO NPs had a deteriorative effect on the Chl content of the green alga *Chlamydomonas reinhardtii* causing photoinhibition of PSII that led to dissipation of energy *via* nonphotochemical pathways. Similarly, Perreault *et al*. (2010) reported that *Lemna gibba,* on exposure to CuO NPs, showed a decrease in q_P with increase in the nonphotochemical quenching. Furthermore, reduction in growth and transpiration of yellow squash (*C. pepo*) was observed after a treatment with nano Cu of size <50 nm (Musante and White 2012). Our results suggest a susceptibility of both light (F_v/F_m) and dark (CO_2 fixation) reactions to CuO NP exposure at high concentrations.

No significant change in the MDA content (Fig. 5*A*) indicated the absence of lipid peroxidation of cell membrane as a result of CuO NP treatment. The increased accumulation of ascorbate in the leaves (Fig. 5*C*) suggested the onset of oxidative response to the CuO NP treatment in the plants. The increased expression of enzymatic antioxidants, APX (Fig. 5*D*) and SOD (Fig. 5*E*), at 10 and 100 mg L^{-1} of CuO NPs, respectively, indicated a protective process against development of oxidative stress in the plants. Accumulation of proline (Fig. 5*B*), an osmoprotectant and a nonenzymatic antioxidant, is an indication of osmotic stress (Alia and Pardha Saradhi 1991) as a result of increasing CuO NP concentration. Osmotic stress in our study was also indicated bymorphological changes, such as increase in the size and number of trichomes and the decrease in the number and size of stomata (Fig. 2*A,B,C*). Proline is one of the widely distributed solutes that is reported to accumulate in plants during adverse stress conditions, such as drought, salinity, high or low temperature (Bohnert *et al*. 1995), or under metal stress (Bassi and Sharma 1993). However, no

accumulation of proline under NP stress has been previously reported. The protective role of proline in mitigating lipid peroxidation upon metal stress was demonstrated in *Chlorella vulgaris* by Mehta and Gaur (1999).

Plant defence mechanisms, such as nonenzymatic (ASA and proline) and enzymatic (APX and SOD) antioxidants, help in mitigating the CuO NP stress. SOD and APX are the key enzymes involved in metabolizing reactive oxygen species (ROS) (Caverzan *et al*. 2012). SOD catalyses the dismutation of $O_2^{-\cdot}$ into H_2O_2 maintaining intracellular $O_2^{-\cdot}$ concentrations (Smirnoff 1993), while APX, which is present mostly in the chloroplast, readily scavenges the hydrogen peroxide produced by SOD into water molecules (Noctor and Foyer 1998). The observed increase in SOD and APX in this study might mitigate an oxidative effect to a certain extent. Studies on the effect of CuO NP on gene expression are few. One such study by Shaw and Hossain (2013) has described enhanced APX and glutathione reductase (GR) activity in rice seedlings as a result of the CuO NP. However, several studies have shown that bulk Cu increases the expression of APX, SOD, and other enzymatic antioxidants in plants (Inzé and van Montagu 1995, Yoshimura *et al*. 2000).

Conclusion: Increasing NP concentrations in the environment affected rice plants. This study highlighted the toxic effects of CuO NPs on the seedling length, morphology, photosynthetic efficiency, and carbon dioxide fixation in *Oryza sativa* var. Jyoti that led to loss of productivity at high concentrations of the pollutant. Uptake of CuO NPs caused a disruption in the number of thylakoids per granum at 50 mg L^{-1} with even stronger structural damage and swelling upon exposure to the higher concentrations. At the same time, there was a decrease in the size and number of stomata but increase in the size and number of trichomes. The evidence suggested an exclusion mechanism for CuO NP at a root level, thereby reducing toxicity in shoots. The study also showed the significant decrease in net CO_2 fixation, in quantum efficiency of PSII (F_v/F_m), increased level of oxidative and osmotic stress, and higher expression of APX and SOD. These findings warrant further investigation of the mechanism of nanoparticle transport within the plant, of ecotoxicological effects on the biochemical parameters, and the potential implications in the food chain.

References

Abdelkader A.F., Aronsson H., Solymosi K. *et al*.: High salt stress induces swollen prothylakoids in dark-grown wheat and alters both prolamellar body transformation and reformation after irradiation. – J. Exp. Bot. **58**: 2553-2564, 2007.

Alia, Pardha Saradhi, P.: Proline accumulation under heavy metal stress. – J. Plant Physiol. **138**: 554-558, 1991.

Bassi R., Sharma S.S.: Changes in proline content accompanying the uptake of zinc and copper by *Lemna minor*. – Ann. Bot.- London **72**: 151-154, 1993.

Bates L.S., Waldren R.P., Teare I.D.: Rapid determination of free proline for water-stress studies. – Plant Soil **39**: 205-207, 1973.

Bohnert H.J., Nelson D.E., Jensen R.G.: Adaptations to environmental stresses. – Plant Cell **7**: 1099-1111, 1995.

Campbell R., Greaves M.P.: Anatomy and community structure of the rhizosphere. – In: Lynch J.M. (ed.): The Rhizosphere. Pp. 11-34. John Wiley and Sons Ltd. Publ., London 1990.

Caverzan A., Passaia G., Rosa S.B. *et al*.: Plant responses to stresses: Role of ascorbate peroxidase in the antioxidant protection. – Genet. Mol. Biol. **35**: 1011-1019, 2012.

Corredor E., Testillano P.S., Coronado M.-J. *et al*.: Nanoparticle penetration and transport in living pumpkin plants: *in situ* subcellular identification. – BMC Plant Biol. **9**: 45-45, 2009.

Harrison P.: Emerging challenges: nanotechnology and the environment. – In: GEO Year Book 2007. Pp. 61-68. United Nations Environment Programme (UNEP), Nairobi 2007.

Haverkamp R.G., Marshall A.T.: The mechanism of metal nanoparticle formation in plants: Limits on accumulation. – J. Nanoparticle Res. **11**: 1453-1463, 2009.

Inzé D., Van Montagu M.: Oxidative stress in plants. – Curr. Opin. Biotech. **6**: 153-158, 1995.

Kampfenkel K., Van Montagu M., Inzé D.: Extraction and determination of ascorbate and dehydroascorbate from plant tissue. – Anal. Biochem. **225**: 165-167, 1995.

Kennedy C.D., Gonsalves F.A.N.: The action of divalent zinc, cadmium, mercury, copper and lead on the trans-root potential and H^+ efflux of excised roots. – J. Exp. Bot. **38**: 800-817, 1987.

Kirchhoff H., Horstmann S., Weis E.: Control of the photosynthetic electron transport by PQ diffusion microdomains in thylakoids of higher plants. – BBA-Bioenergetics **1459**: 148-168, 2000.

Klaine S.J., Alvarez P.J.J., Batley G.E. *et al*.: Nanomaterials in the environment: behavior, fate, bioavailability, and effects. – Environ. Toxicol. Chem. **27**: 1825-1851, 2008.

Lee C.W., Mahendra S., Zodrow K. *et al*.: Developmental phytotoxicity of metal oxide nanoparticles to *Arabidopsis thaliana*. – Environ. Toxicol. Chem. **29**: 669-675, 2010.

Lee S., Kim S., Kim S. *et al*.: Assessment of phytotoxicity of ZnO NPs on a medicinal plant, *Fagopyrum esculentum*. – Environ. Sci. Pollut. Res. **20**: 848-854, 2013.

Lee W.M., An Y.J., Yoon H. *et al*.: Toxicity and bioavailability of copper nanoparticles to the terrestrial plants mung bean (*Phaseolus radiatus*) and wheat (*Triticum aestivum*): plant agar test for water-insoluble nanoparticles. – Environ. Toxicol. Chem. **27**: 1915-1921, 2008.

Lidon F.C., Henriques F.S.: Role of rice shoot vacuoles in

copper toxicity regulation. – Environ. Exp. Bot. **39**: 197-202, 1998.

Lin D., Xing B.: Root uptake and phytotoxicity of ZnO nanoparticles. – Environ. Sci. Technol. **42**: 5580-5585, 2008.

Manceau A., Nagy K.L., Marcus M.A. *et al*.: Formation of metallic copper nanoparticles at the soil-root interface. – Environ. Sci. Technol. **42**: 1766-1772, 2008.

Marschner H.: Mineral Nutrition of Higher Plants. Pp. 889. Academic Press, London 1995.

Maynard A.D., Aitken R.J., Butz T. *et al*.: Safe handling of nanotechnology. – Nature **444**: 267-269, 2006.

Mehta S.K., Gaur J.P.: Heavy metal-induced proline accumulation and its role in ameliorating metal toxicity in *Chlorella vulgaris*. – New Phytol. **143**: 253-259, 1999.

Musante C., White J.C.: Toxicity of silver and copper to *Cucurbita pepo*: Differential effects of nano and bulk-size particles. – Environ. Toxicol. **27**: 510-517, 2012.

Nagajyoti P.C., Lee K.D., Sreekanth T.V.M. *et al*.: Heavy metals, occurrence and toxicity for plants: A review. – Environ. Chem. Lett. **8**: 199-216, 2010.

Navarro E., Baun A., Behra R. *et al*.: Environmental behavior and ecotoxicity of engineered nanoparticles to algae, plants, and fungi. – Ecotoxicology **5**: 372-386, 2008.

Nekrasova G.F., Ushakova O.S., Ermakov A.E. *et al*.: Effects of copper (II) ions and copper oxide nanoparticles on *Elodea densa* Planch. – Russian J. Ecol. **42**: 458-463, 2011.

Noctor G., Foyer C.H.: Ascorbate and glutathione: Keeping active oxygen under control. – Annu. Rev. Plant Phys. **49**: 249-279, 1998.

Ojamäe L., Aulin C., Pedersen H. *et al*.: IR and quantum-chemical studies of carboxylic acid and glycine adsorption on rutile TiO_2 nanoparticles. – J. Colloid Interface Sci. **296**: 71-78, 2006.

Perreault F., Oukarroum A., Pirastru L. *et al*.: Evaluation of copper oxide nanoparticles toxicity using chlorophyll a fluorescence imaging in *Lemna gibba*. – J. Bot. **2010**, 1-9, 2010.

Raven J.A., Evans M.C., Korb R.E.: The role of trace metals in photosynthetic electron transport in O_2 – evolving organisms. – Photosynth. Res. **60**: 111-150, 1999.

Rico C.M., Majumdar S., Duarte-Gardea M. *et al*.: Interaction of nanoparticles with edible plants and their possible implications in the food chain. – J. Agric. Food Chem. **59**: 3485-3498, 2011.

Saison C., Perreault F., Daigle J.C. *et al*.: Effect of core-shell copper oxide nanoparticles on cell culture morphology and photosynthesis (photosystem II energy distribution) in the green alga, *Chlamydomonas reinhardtii*. – Aquat. Toxicol. **96**: 109-114, 2010.

Sankhalkar S., Sharma P.K.: Protection against photooxidative damage provided by enzymatic and non-enzymatic anti-oxidant system in sorghum seedlings. – Indian J. Exp. Biol. **40**: 1260-1268, 2002.

Sharma P.K., Hall D.O.: Effect of photoinhibition and temperature on carotenoids in sorghum leaves. – Indian J. Biochem. Biophys. **33**: 471-477, 1996.

Sharma P.K., Shetye R., Bhonsle S.: Effect of supplementary ultraviolet-B radiation on young wheat seedlings. – Curr. Sci. **72**: 400-405, 1997.

Shaw A.K., Hossain Z.: Impact of nano-CuO stress on rice (*Oryza sativa* L.) seedlings. – Chemosphere **93**: 906-915, 2013.

Shi J., Abid A.D., Kennedy I.M. *et al*.: To duckweeds (*Landoltia punctata*), nanoparticulate copper oxide is more inhibitory than the soluble copper in the bulk solution. – Environ. Pollut. **159**: 1277-1282, 2011.

Smirnoff N.: Tansley Review 52. The role of active oxygen in the response of plants to water-deficit and desiccation. – New Phytol. **125**: 27-58, 1993.

Solymosi K., Bertrand M.: Soil metals, chloroplasts, and secure crop production: a review. – Agron. Sustain. Dev. **32**: 245-272, 2012.

Song, L., Vijver, M. G., Peijnenburg, W. J. G. M.: Comparative toxicity of copper nanoparticles across three Lemnaceae species. – Sci. Total Environ. **518-519**: 217-224, 2015.

Stampoulis D., Sinha S.K., White J.C.: Assay-dependent phytotoxicity of nanoparticles to plants. – Environ. Sci. Technol. **43**: 9473-9479, 2009.

Ünnep R., Zsiros O., Solymosi K. *et al*.: The ultrastructure and flexibility of thylakoid membranes in leaves and isolated chloroplasts as revealed by small-angle neutron scattering. – BBA- Bioenergetics **1837**: 1572-1580, 2014.

Wang S.-H., Yang Z.-M., Yang H. *et al.*: Copper-induced stress and antioxidative responses in roots of *Brassica juncea* L. – Bot. Bull. Acad. Sin. **45**: 203-212, 2004.

Wierzbicka M.S., Obidzińska J.: The effect of lead on seed imbibition and germination in different plant species. – Plant Sci. **137**: 155-171, 1998.

Wiesner M.R., Lowry G.V., Alvarez P. *et al.*: Assessing the risks of manufactured nanomaterials. – Environ. Sci. Technol. **40**: 4336-4345, 2006.

Yoshimura K., Yabuta Y., Ishikawa T. *et al*.: Expression of spinach ascorbate peroxidase isoenzymes in response to oxidative stresses. – Plant Physiol. **123**: 223-233, 2000.

Yruela I.: Copper in plants. – Brazilian J. Plant Physiol. **17**: 145-156, 2005.

Zhang W., Elliott D.W.: Applications of iron nanoparticles for groundwater remediation. – Remediat. J. **16**: 7-21, 2006.

Zhang Z., He X., Zhang H. *et al*.: Uptake and distribution of ceria nanoparticles in cucumber plants. – Metallomics **3**: 816-822, 2011.